Available online at www.sciencedirect.com
SCIENCE DIRECT®
Nuclear Instruments and Methods in Physics Research A 560 (2006) 240–244
NUCLEAR INSTRUMENTS & METHODS IN PHYSICS RESEARCH Section A
www.elsevier.com/locate/nima

Inhomogeneous effects in the quantum free electron laser

N. Piovella[a,b,*], R. Bonifacio[b,c]

[a]Dipartimento di Fisica and INFM, Università Degli Studi di Milano, Via Celoria 16, I-20133 Milano, Italy
[b]INFN—Sezione di Milano, Via Celoria 16, I-20133 Milano, Italy
[c]Departemento di Fisica, Universidade Federal Alagoas, Maceiò, 57072-970, Brazil

Received 23 January 2006; accepted 25 January 2006
Available online 24 February 2006

Abstract

We include inhomogeneous effects in the quantum model of a free electron laser taking into account the initial energy spread of the electron beam. From a linear analysis, we obtain a generalized dispersion relation, from which the exponential gain can be explicitly calculated. We determine the maximum allowed initial energy spread in the quantum exponential regime and we discuss the limit of large energy spread.

PACS: 41.60.Cr; 42.50.Fx

Keywords: FEL; SASE; Quantum recoil

1. Introduction

Recently a new quantum regime of high-gain free electron lasers (FELs) has been proposed [1–3], particularly attractive for the realization of a coherent X-ray source based on Self Amplified Spontaneous Emission (SASE) operation [4]. The realization of an FEL source in the Angstrom region and based on classical SASE is currently the subject of intense experimental effort [5,6]. However, the radiation spectrum produced by classical SASE is broad, and the output radiation is a random superposition of many superradiant spikes, of the order of the number of cooperation lengths contained in the electron beam length [7]. Conversely, it has been predicted [2] that in the quantum SASE regime (i.e. in the quantum regime starting from noise) the temporal coherence of the output radiation is greatly enhanced, and the spectrum is composed by a single or few narrow lines [8].

The transition from the classical regime to the quantum regime in an FEL occurs when the photon recoil momentum $\hbar k$ becomes larger than the induced electron energy spread. Since the maximum energy spread at saturation is approximately $mc^2\gamma\rho$, where ρ is the classical BPN parameter [4], then an FEL is in the quantum regime when

$$\bar{\rho} = \rho \frac{mc\gamma}{\hbar k} < 1. \tag{1}$$

For $\bar{\rho} \gg 1$ the discreteness of the photon recoil can be neglected and the electron momentum decreases continuously by recoil, so that the electron motion can be described classically. On the contrary, for $\bar{\rho} < 1$ the electron momentum decreases by discrete steps of $\hbar k$ and a quantum-mechanical treatment of the electron dynamics shows the existence of a completely different regime in which each electron emits coherently a single photon [1].

In this paper, we extend the results of the quantum FEL model discussed in Ref. [2] to include the inhomogeneous effects due to the broadening of the resonance, caused by for instance a spread of the initial electron energy. The significance of the inclusion of inhomogeneous effects is that it allows us obtain an upper limit for the initial energy

*Corresponding author. Dipartimento di Fisica and INFM, Università Degli Studi di Milano, Via Celoria 16, I-20133 Milano, Italy. Tel.: +390250317266; fax: +390250317675.
E-mail address: nicola.piovella@mi.infn.it (N. Piovella).

0168-9002/$ - see front matter
doi:10.1016/j.nima.2006.01.128

spread in the electron beam driving an FEL in the quantum regime.

2. Inhomogeneous quantum FEL model

It has been proposed [2,3,9] that the Quantum FEL (QFEL) is described by the following equations for the dimensionless radiation amplitude $A(\bar{z}, z_1)$ and the electron wave function $\Psi(\theta, \bar{z}, z_1)$:

$$i\frac{\partial \Psi}{\partial \bar{z}} = -\frac{1}{2\bar{\rho}}\frac{\partial^2}{\partial \theta^2}\Psi - i\bar{\rho}[Ae^{i\theta} - \text{c.c.}]\Psi \tag{2}$$

$$\frac{\partial A}{\partial \bar{z}} + \frac{\partial A}{\partial z_1} = \frac{1}{2\pi}\int_0^{2\pi} d\theta |\Psi|^2 e^{-i\theta} + i\delta A. \tag{3}$$

The notations are the same of Refs. [2,7]. In particular, $\bar{z} = z/l_g$ is the coordinate along the wiggler (in units of the gain length $l_g = \lambda_w/4\pi\rho$), $\theta = (k + k_w)z - ckt$ is the electron phase, $z_1 = (z - c\beta_r)/\beta_r l_c$ is the coordinate along the electron bunch (in units of the cooperation length $l_c = \lambda/4\pi\rho$), A is the dimensionless field amplitude, such that $\bar{\rho}|A|^2$ is the ratio between the photon density and the electron density, $\delta = (\gamma_0 - \gamma_r)/\rho\gamma_r$ is the normalized detuning parameter, γ_0 and $\gamma_r = \sqrt{k(1 + a_w^2)/2k_w}$ are the initial and resonant electron energies in mc^2 units, respectively, $\beta_r = v_r/c$, and v_r is the resonant electron velocity.

The QFEL model of Eqs. (2) and (3) was obtained in Ref. [3] using a multiple-scale approach, previously applied to classical FEL theory [10]. The method exploits the existence of two different spatial scales: the variation of the electron distribution on the scale of the radiation wavelength λ (describing the bunching) and the variation of the field envelope on the much longer scale of the cooperation length l_c. As discussed previously [1], Eqs. (2) and (3) depend on the single dimensionless parameter, $\bar{\rho}$, ruling the transition between the classical ($\bar{\rho} \gg 1$) and quantum ($\bar{\rho} < 1$) regimes.

Eqs. (2) and (3) have been derived assuming a monoenergetic electron beam. More precisely, the parameter δ describes the detuning of the initial electron energy γ_0 from the resonant energy γ_r, defined by the central frequency $\omega = ck$ of the emitted radiation. The model of Eqs. (2) and (3) can be generalized to take into account for inhomogeneous broadening: different electrons may have different detunings δ, i.e. different initial energies and/or different resonant energies, distributed by a function $G_0(\delta)$.

The effect of a distribution $G_0(\delta)$ (describing different classes of electrons, each one with its own detuning δ), is more conveniently included in the model of Eqs. (2) and (3) where $\Psi(\theta, \bar{z}, \bar{z}_1)$ (assumed to be a periodic function of θ) is expanded in a Fourier series:

$$\Psi(\theta, \bar{z}, z_1) = \sum_{n=-\infty}^{\infty} c_n(\bar{z}, z_1) e^{in(\theta + \delta\bar{z})}. \tag{4}$$

The coefficient $c_n(\bar{z}, z_1, \delta)$ can be interpreted quantum-mechanically as the probability amplitude to find an electron with a detuning δ and a momentum $p = n(\hbar k)$. In fact, Eq. (4) is the expansion of the electron wave function on the basis of p with eigenstates $\exp(in\theta)$ and eigenvalues $n(\hbar k)$.

Inserting Eq. (4) into Eqs. (2) and (3), defining $A = \bar{A}e^{i\delta\bar{z}}$ and generalizing the source term of Eq. (3) to include all the different detunings δ weighted by $G_0(\delta)$, we obtain

$$\frac{\partial c_n}{\partial \bar{z}} = -in\left(\frac{n}{2\bar{\rho}} + \delta\right)c_n - \bar{\rho}[\bar{A}c_{n-1} - \bar{A}^* c_{n+1}] \tag{5}$$

$$\frac{\partial \bar{A}}{\partial \bar{z}} + \frac{\partial \bar{A}}{\partial z_1} = \sum_{n=-\infty}^{\infty}\int_{-\infty}^{\infty} d\delta G_0(\delta)\, c_{n-1}^* c_n. \tag{6}$$

The term on the right-hand side of Eq. (6) is the quantum expression for the local bunching, $b(\bar{z}, z_1) = \langle e^{-i\theta}\rangle = \int d\delta G_0(\delta)\sum_n c_{n-1}^*(\delta)c_n(\delta)$ and shows that lasing is possible only in the presence of a coherent superposition of two adjacent momentum states of electrons at the position z_1.

3. Linear analysis

We perform a stability analysis of Eqs. (5) and (6) of the initial equilibrium state with no field, $\bar{A} = 0$, and all the electrons in the same momentum state n, i.e. $c_n = e^{i\omega_n\bar{z}}$ and $c_m = 0$ for $m \neq n$, where $\omega_n = n(n/2\bar{\rho} + \delta)$ are the eigenvalues of the system. Linearizing Eqs. (5) and (6) around this equilibrium state and defining $a_1 = c_{n-1}^* e^{-i\omega_n\bar{z}}$ and $a_2 = c_{n+1}e^{i\omega_n\bar{z}}$, we obtain

$$\frac{\partial a_1}{\partial \bar{z}} = -i\left(\delta_n - \frac{1}{2\bar{\rho}}\right)a_1 + \bar{\rho}\bar{A} \tag{7}$$

$$\frac{\partial a_2}{\partial \bar{z}} = -i\left(\delta_n + \frac{1}{2\bar{\rho}}\right)a_2 - \bar{\rho}\bar{A} \tag{8}$$

$$\frac{\partial \bar{A}}{\partial \bar{z}} + \frac{\partial \bar{A}}{\partial z_1} = \int_{-\infty}^{+\infty} d\delta G_0(\delta)[a_1 + a_2] \tag{9}$$

where $\delta_n = \delta + n/\bar{\rho}$. Introducing the Laplace transform in $\bar{z}$ and the Fourier transform in z_1,

$$\tilde{f}(\bar{k}, \lambda) = \frac{1}{2\pi}\int_{-\infty}^{\infty} dz_1 \int_0^{\infty} d\bar{z} f(z_1, \bar{z}) e^{-i(\bar{k}z_1 + \lambda\bar{z})} \tag{10}$$

and assuming $a_1(z_1, 0) = a_2(z_1, 0) = 0$ for a continuous beam and $\bar{A}(z_1, 0) = A_0(z_1)$, Eqs. (7)–(9) yield

$$\tilde{A}(\bar{k}, \lambda) = -i\frac{\tilde{A}_0(\bar{k})}{D(\bar{k}, \lambda)} \tag{11}$$

where

$$D(\bar{k}, \lambda) = \lambda - \bar{k} + \int_{-\infty}^{+\infty} d\delta \frac{G_0(\delta)}{(\lambda + \delta_n)^2 - 1/4\bar{\rho}^2}. \tag{12}$$

Then, the Fourier transform of the radiation field is

$$\tilde{A}(\bar{k}, \bar{z}) = \tilde{A}_0(\bar{k})\tilde{F}(\bar{k}, \bar{z}) \tag{13}$$

where

$$\tilde{F}(\bar{k}, \bar{z}) = \sum \text{Res}\left\{\frac{e^{i\lambda\bar{z}}}{D(\bar{k}, \lambda)}\right\} \tag{14}$$

and the spatial growth modes λ are given by the roots of the dispersion equation $D(\bar{k}, \lambda) = 0$. Assuming $G_0(\delta)$ centered around $\bar{\delta}_n = \bar{\delta} + n/\bar{\rho}$ and defining $\omega = \lambda + \bar{\delta}_n$

and $\delta' = \delta - \bar{\delta}_n$, the dispersion equation becomes

$$\omega - \Delta + \int_{-\infty}^{+\infty} \mathrm{d}\delta' \frac{G_0(\delta')}{(\omega+\delta')^2 - 1/4\bar{\rho}^2} = 0 \tag{15}$$

where $\Delta = \bar{\delta} + n/\bar{\rho} - \bar{k}$ is the generalized detuning. Eq. (15) can be written also in the following form:

$$\omega - \Delta + \bar{\rho} \int_{-\infty}^{+\infty} \frac{\mathrm{d}\delta'}{\omega+\delta'} \left[G_0\left(\delta' + \frac{1}{2\bar{\rho}}\right) - G_0\left(\delta' - \frac{1}{2\bar{\rho}}\right) \right] = 0. \tag{16}$$

Note that the same dispersion equation (16) can be obtained linearizing the Wigner model for QFEL (see Ref. [3], Eqs. (20) and (21)), where $G_0(\bar{p}) = (1/2\pi)\int_{-\infty}^{\infty} \mathrm{d}\theta W(\theta, \bar{p}, z_1, 0)$ is the marginal distribution in $\bar{p}$ of the Wigner function $W(\theta, \bar{p}, z_1, \bar{z} = 0)$ (supposed initially uniform and unbunched) and $\bar{p} = (\gamma - \gamma_0)/\rho\gamma_r$.

In the classical limit, $\bar{\rho} \gg 1$, the finite difference $\bar{\rho}[G_0(\delta' + 1/2\bar{\rho}) - G_0(\delta' - 1/2\bar{\rho})]$ in Eq. (16) tends to the derivative $\mathrm{d}G_0(\delta')/d\delta'$, so that, after an integration by parts, Eq. (16) becomes the well known classical relation [11]:

$$\omega - \Delta + \int_{-\infty}^{+\infty} \frac{\mathrm{d}\delta'}{(\omega+\delta')} \left(\frac{\mathrm{d}G_0}{\mathrm{d}\delta'}\right) = 0 \tag{17}$$

as can be obviously obtained also from Eq. (15).

Note that from Eq. (11) it is possible even to obtain the solution of the field in the time domain,

$$\bar{A}(z_1, z_2) = \int_{-\infty}^{\infty} \mathrm{d}z_1' A_0(z_1') F(z_1 - z_1', z_2) \tag{18}$$

where

$$F(z_1, z_2) = \mathrm{e}^{-\mathrm{i}\delta_n z_2} \oint \mathrm{d}\omega\, \mathrm{e}^{\mathrm{i}\omega z_2 - \mathrm{i}z_1 \int \mathrm{d}\delta G_0(\delta)/((\omega+\delta)^2 - 1/4\bar{\rho}^2)}, \tag{19}$$

for $z_2 > 0$ and zero elsewhere, where $z_2 = \bar{z} - z_1 = (ct - z)/l_c$ and the complex integral in (19) surrounds all the essential singularities of the exponential function. The explicit solution in the classical limit and in the case of a mono-energetic beam has been calculated in Ref. [12], whereas the general solution of (19) will be discussed elsewhere.

4. Large broadening case

In the case of a very broad distribution $G_0(\delta)$, the imaginary part of the solution ω of the dispersion equation (16) is small. Hence, using the limit

$$\lim_{\varepsilon\to 0}\left(\frac{1}{x + \mathrm{i}\varepsilon}\right) = P\left(\frac{1}{x}\right) - \mathrm{i}\pi\delta(x)$$

in the integral on δ' of Eq. (16), where $x = \mathrm{Re}\,\omega + \delta'$, $\varepsilon = \mathrm{Im}\,\omega$ and P is the principal part, we obtain $\mathrm{Re}\,\omega \approx \Delta$ and

$$G \approx -2\,\mathrm{Im}\,\omega \approx 2\pi\bar{\rho}\left[G_0\left(\Delta - \frac{1}{2\bar{\rho}}\right) - G_0\left(\Delta + \frac{1}{2\bar{\rho}}\right)\right] \tag{20}$$

where we assumed G_0 to be a symmetric function around zero. We see from Eq. (20) that in the classical limit, $\bar{\rho} \gg 1$, and for large broadening, $\sigma \gg 1$ (where σ is the width of G_0), the gain is $G \approx -(2\pi)\,\mathrm{d}G_0(\Delta)/\mathrm{d}\Delta$. Instead, in the quantum limit, $\bar{\rho} < 1$, the gain is the difference between the distribution G_0 centered around $\Delta = 1/\bar{\rho}$ (emission) and the one centered around $\Delta = -1/\bar{\rho}$ (absorbtion). Eq. (20) yields the maximum gain at $\Delta = 1/2\bar{\rho}$,

$$G_{\max} \approx 2\pi\bar{\rho}\left[G_0(0) - G_0\left(\frac{1}{\bar{\rho}}\right)\right] \tag{21}$$

which shows that the maximum gain in the quantum regime decreases for $\sigma \gg 1/\bar{\rho}$, i.e. $mc(\delta\gamma) \gg \hbar k$. This condition set an upper limit to the initial momentum spread $mc(\delta\gamma)$, which must be less than the photon momentum $\hbar k$, i.e. less than the separation of the two momentum levels $n = 0$ and $n = -1$. In fact, an initial momentum distribution larger than $\hbar k$ cannot resolve the quantum transition between the two momentum states. The quantum expression (20) is valid for σ much larger than the resonant gain (which will be calculated in the next section). If σ is also much smaller than $1/\bar{\rho}$, i.e. if the momentum spread is smaller than the photon recoil momentum $\hbar k$, the absorbtion term in Eq. (20) (proportional to $G_0(\Delta + 1/2\bar{\rho})$) can be neglected and the gain in the large broadening quantum regime is a symmetric function of Δ around the resonance value $\Delta = 1/\bar{\rho}$:

$$G \approx 2\pi\bar{\rho}\, G_0\left(\Delta - \frac{1}{2\bar{\rho}}\right). \tag{22}$$

5. A special case: the Lorentzian distribution

In general, the exact solution of the dispersion relation (15) for a given $G_0(\delta)$ can be obtained only numerically. However, in the case of a Lorentzian distribution, $G_0(\delta) = (1/\pi)[\sigma/(\sigma^2 + \delta^2)]$, the integral in Eq. (15) can be calculated analytically, giving the following cubic equation:

$$(\omega - \Delta)\left[(\omega - \mathrm{i}\sigma)^2 - \frac{1}{4\bar{\rho}^2}\right] + 1 = 0. \tag{23}$$

Fig. 1 shows the gain $G = -2\,\mathrm{Im}\,\omega$ as a function of Δ for two large-spread cases, calculated from Eq. (23): the first corresponds to the classical regime (dashed line (a), with $\bar{\rho} = 5$ and $\sigma = 2$), whereas the second corresponds to the quantum regime (continuous line (b), with $\bar{\rho} = 0.1$ and $\sigma = 1$). In the classical case the gain has an antisymmetric shape around $\Delta \approx 0$ and it is approximately proportional to the derivative of the distribution function $G_0(\Delta)$. On the contrary, in the quantum regime the gain is symmetric around the quantum resonance $\Delta = 1/2\bar{\rho}$, whereas absorbtion occurs around $\Delta = -1/2\bar{\rho}$. As discussed in the previous section, the gain is proportional to the difference between the emission and absorbtion lineshapes, separated by the recoil momentum $\hbar k$ ($1/\bar{\rho}$ in our dimensionless

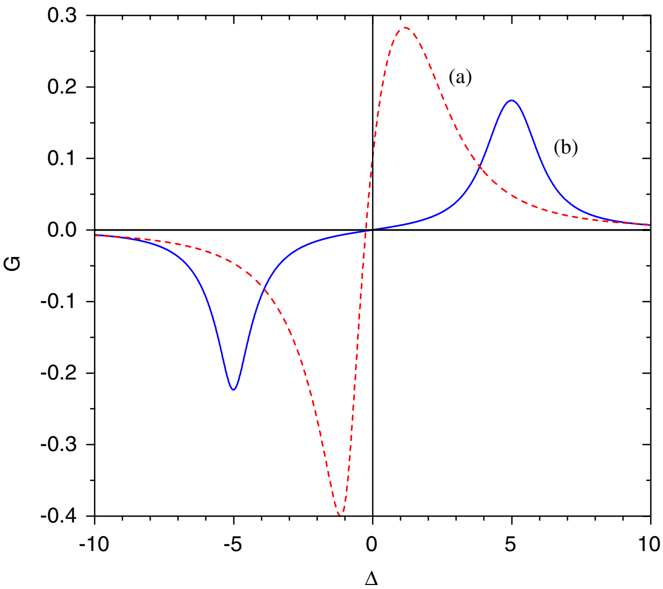

Fig. 1. Gain shape in the classical regime, dashed line (a), for $\bar{\rho}=5$ and $\sigma=2$, and in the quantum regime, continuous line (b), for $\bar{\rho}=0.1$ and $\sigma=1$.

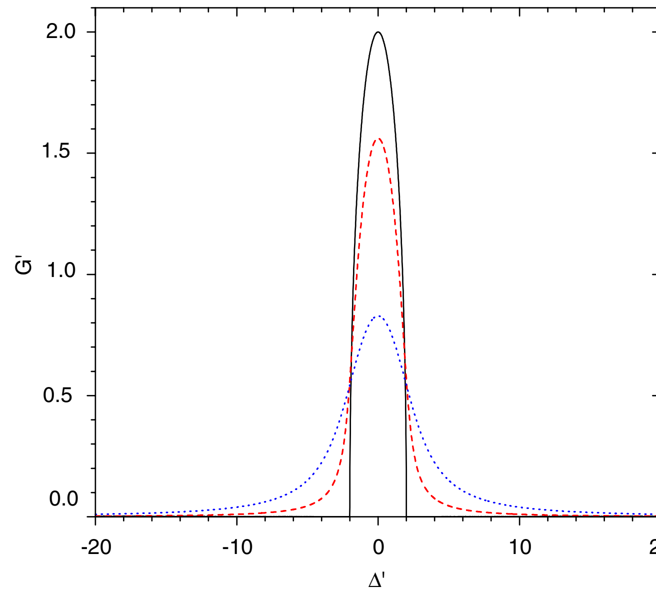

Fig. 2. Gain shape in the quantum regime. Here $G'=G/\sqrt{\bar{\rho}}$ and $\Delta'=(\Delta-1/2\bar{\rho})/\sqrt{\bar{\rho}}$. The different values of the spread are $\sigma'=0$ (continuous line), $\sigma'=0.5$ (dashed line) and $\sigma'=2$ (dotted line), where $\sigma'=\sigma/\sqrt{\bar{\rho}}$.

variables). In the quantum regime the emission and absorbtion rates are well separated (if $\sigma \ll 1/\bar{\rho}$), so that, around $\Delta=1/2\bar{\rho}$, the absorbtion can be neglected and the gain has a symmetric shape. In the quantum regime, $\bar{\rho}\ll 1$, the three roots of the cubic (23) can be evaluated approximately as

$$\omega_1 \approx \frac{1}{2\bar{\rho}}+\frac{\sqrt{\bar{\rho}}\Delta'}{2}\left(1+\frac{\sigma'}{B}\right)-\mathrm{i}\frac{\sqrt{\bar{\rho}}}{2}(B-\sigma') \tag{24}$$

$$\omega_2 \approx \frac{1}{2\bar{\rho}}+\frac{\sqrt{\bar{\rho}}\Delta'}{2}\left(1-\frac{\sigma'}{B}\right)+\mathrm{i}\frac{\sqrt{\bar{\rho}}}{2}(B+\sigma') \tag{25}$$

$$\omega_3 \approx \frac{1}{2\bar{\rho}}+\mathrm{i}\sqrt{\bar{\rho}}\sigma' \tag{26}$$

where $\Delta'=(\Delta-1/2\bar{\rho})/\sqrt{\bar{\rho}}$, $\sigma'=\sigma/\sqrt{\bar{\rho}}$ and

$$B=\left[\frac{\sqrt{(4+\sigma'^2-\Delta'^2)^2+(2\Delta'\sigma')^2}+4+\sigma'^2-\Delta'^2}{2}\right]^{1/2}. \tag{27}$$

Hence, the gain $G=-2\,\mathrm{Im}\,\omega_1=\sqrt{\bar{\rho}}(B-\sigma')$ is maximum at resonance $\Delta'=0$ (i.e. for $\Delta=1/2\bar{\rho}$), with

$$G_{\max}=\sqrt{\bar{\rho}}\left[\sqrt{4+\sigma'^2}-\sigma'\right]. \tag{28}$$

Note that for $\sigma'\ll 2$, $G_{\max}\approx 2\sqrt{\bar{\rho}}[1-\sigma'/2+\sigma'^2/8]$, whereas for $\sigma'\gg 2$, $G_{\max}\approx 2\bar{\rho}/\sigma$, in agreement with Eq. (22). Fig. 2 shows $G'=G/\sqrt{\bar{\rho}}$ in the quantum regime, for $\sigma'=0$ (continuous line), $\sigma'=0.5$ (dashed line) and $\sigma'=2$ (dotted line). The exact solution of Eq. (23) agrees with the approximated solution of Eqs. (24) and (27) for $\bar{\rho}\ll 1$. Note that, from Eq. (27), the full bandwidth of the gain is approximately equal to $\sigma_{\Delta'}\approx 2\sqrt{4+\sigma'^2}$. Hence, the gain bandwidth is $\sigma_\Delta=4\sqrt{\bar{\rho}}$ for $\sigma=0$ and increases linearly with σ when σ is much larger than $\sqrt{\bar{\rho}}$ (but always smaller than the quantum limit $1/\bar{\rho}$).

6. Discussion and conclusions

We have presented analytical results about the effects of the inhomogeneous broadening of the resonance in a QFEL. The complete analysis of the nonlinear equations (5) and (6) will be discussed in a future extended paper. However, it is already possible to obtain from the results presented here a criterium for the initial electron energy spread needed to lase, together with some spectral features of the SASE regime in QFEL. The linear analysis shows that the quantum regime (i.e. the reduction to only two momentum states) requires $\sigma\ll 1/\bar{\rho}$, i.e. the initial energy spread must be $\delta\gamma\ll\lambda_C/\lambda$, where $\lambda_C=h/mc\approx 0.024\,\text{Å}$ is the Compton wavelength and λ is the lasing radiation wavelength. In order to lase at $\lambda\sim 1\,\text{Å}$ using a static wiggler as in the classical SASE-FEL experiments [6], then $\gamma_r\sim 10^4$ and $\delta\gamma/\gamma_r\ll 10^{-6}$, which is prohibitively small. On the contrary, using a laser wiggler with $\lambda_w\sim 1\,\mu\mathrm{m}$ [13,14], then $\gamma_r\sim 10^2$ and $\delta\gamma/\gamma_r\ll 10^{-4}$, which is experimentally accessible. However, the criterium $\sigma\ll 1/\bar{\rho}$ sets only a necessary condition on the energy spread: to lase a large number of photons (of the order of the number of electrons in the bunch), the energy spread must be smaller than the homogeneous gain bandwidth, $\sigma\leqslant 4\sqrt{\bar{\rho}}\ll 1/\bar{\rho}$, i.e. $\delta\gamma/\gamma_r\leqslant 4\rho\sqrt{\bar{\rho}}\ll(\rho/\bar{\rho})$. The last inequality implies that $\bar{\rho}$ must be less than $(1/2)^{4/3}\approx 0.4$ in order to lase in the quantum regime.

From the present linear analysis we obtain also an important feature of the SASE regime of QFEL: the radiation spectrum is centered around the resonance $\Delta = 1/2\bar{\rho}$. which for SASE implies that the radiation spectrum is composed by discrete lines at dimensionless frequency $\bar{k} = -(1-2n)/(2\bar{\rho})$, where $n = 0, -1, \ldots$ [8]. Hence, the discrete frequency generated in QFEL are $ck_n = ck - (1-2n)\omega_{\rm rec}$, where $\omega_{\rm rec} = \hbar k^2/2m\gamma_{\rm r}$ is the relativistic recoil frequency. Finally, the spectral line width is $\delta\omega/\omega \approx 2\rho(4\bar{\rho} + \sigma^2)^{1/2}$. These results are limited to the linear regime. A more complete analysis of the energy spread effects and of the spectral properties of the SASE radiation in QFEL in the nonlinear regime will be discussed elsewhere.

Acknowledgments

We thank G.R.M. Robb for a careful reading of the manuscript and for helpful discussions.

References

[1] R. Bonifacio, M.M. Cola, N. Piovella, G.R.M. Robb, Europhys. Lett. 69 (2005) 55.
[2] R. Bonifacio, N. Piovella, G.R.M. Robb, Nucl. Instr. and Meth. A 543 (2005) 645.
[3] R. Bonifacio, N. Piovella, G.R.M. Robb, M.M. Cola, Opt. Commun. 252 (2005) 381.
[4] R. Bonifacio, C. Pellegrini, L. Narducci, Opt. Commun. 50 (1984) 373.
[5] J. Andruszkow, et al., Phys. Rev. Lett. 85 (2000) 3825.
[6] S.V. Milton, et al., Science 292 (2001) 2037.
[7] R. Bonifacio, L. De Salvo, P. Pierini, N. Piovella, C. Pellegrini, Phys. Rev. Lett. 73 (1994) 70.
[8] R. Bonifacio, N. Piovella, G.R.M. Robb, Proceedings of the 27th International Free Electron Laser Conference, Stanford, CA, August 21–26, 2005.
[9] G. Preparata, Phys. Rev. A 38 (1988) 233.
[10] G.T. Moore, M.O. Scully, Phys. Rev. A 21 (1980) 2000.
[11] R. Bonifacio, F. Casagrande, G. Cerchioni, L. De Salvo Souza, P. Pierini, N. Piovella, Riv. Nuovo Cimento 13 (9) (1990).
[12] R. Bonifacio, L. De Salvo Souza, P. Pierini, N. Piovella, Nucl. Instr. and Meth. A 296 (1990) 358.
[13] R. Bonifacio, Nucl. Instr. and Meth. A 546 (2005) 634.
[14] R. Bonifacio, M. Ferrario, G.R.M. Robb, N. Piovella, A. Schiavi, L. Serafini, Proceedings of the 27th International Free Electron Laser Conference, Stanford, CA, August 21–26, 2005.